Colloidal dynamics: influence of diffusion, inertia and colloidal forces on cluster formation

Nina Kovalchuk[1,2], Victor Starov[1f], Paul Langston[3], Nidal Hilal[3], Viacheslav Zhdanov[4]

[1] *Department of Chemical Engineering, Loughborough University, Loughborough, LE11 3TU (UK)*

[2]*Institute of Biocolloid Chemistry, 03142 Kiev, Ukraine*

[3] *School of Chemical, and Environmental Engineering, University of Nottingham, University Park, Nottingham, NG7 2RD (UK)*

[4]*Moscow State University of Food Production, 11 Volokolamskoe sh., Moscow, 125080, Russia*

Abstract

Computer simulations of colloidal suspensions are discussed. The simulations are based on the Langevin equations, pairwise interaction between colloidal particles and take into account Brownian, hydrodynamic and colloidal forces. Comparison of two models, one taking into accout inertial term in Langevin equation and other based on diffusional approximation proposed in Ermak D.L., and McCammon J.A. *J. Chem. Phys*., 1978, **69**, 1352 have shown that both models the prediction of the correct values of the diffusion coefficient and residence time of particle in a doublet and ere therefore suitable to study the dynamics of formation and breakage of clusters in colloidal suspensions. It is shown that the appropriate selection of the time step and taking into account inertia of particles provides also the correct value of the average kinetic energy of each particle during the simulations, what allows to use the model based on full Langevin equations as a reference model to verify the validity of the numerical scheme for simulation using diffusion approximation.

Key words: colloidal suspensions, Langevin equations, colloidal forces, Brownian forces, hydrodynamic interactions, fluctuation-dissipation theorem, clusters.

[f] Corresponding author: V.M.Starov@lboro.ac.uk

Introduction

Stability is the most important characteristic of colloidal suspensions. It is determined by the balance of forces acting between the colloidal particles in the suspension, that is, by the potential of colloidal interaction between particles. DLVO theory and recent modifications of that theory (including Derjaguin's structural forces) are used to describe colloidal interactions between particles [1, 2]. We use a modified DLVO theory to include those forces. Derjaguin's approximation [1] is usually used to calculate forces between colloidal particles. This approximation is applicable if the radius of action of colloidal forces is much smaller than the particle radius, a. The latter condition is satisfied in the case of $a \sim 1\ \mu m$, which is under consideration here. According to the modified DLVO theory [1, 2] colloidal forces are determined by three major components: (i) dispersion forces, (ii) electrostatic forces and (iii) "Derjaguin's" structural forces, which are due to the water dipoles orientation. Here we use "structural forces" just in this sense. In the case of identical particles dispersion forces always result in attraction and electrostatic forces in repulsion between particles. The influence of structural forces is still under debate. The presence of an electrical charge at the particles surfaces and electrical double layer, as well as structural repulsion, stabilises the suspension due to appearance of the potential barrier preventing their coagulation in the primary potential well [1, 2].

Stable suspensions are usually considered as built up by uniformly distributed single particles, whereas clustering is regarded as an attribute of thermodynamically and kinetically unstable suspensions undergoing irreversible coagulation. However, comprehensive experimental studies performed during recent years discovered the existence of stable clusters in colloidal suspensions stabilised by electrostatic and/or structural repulsion [3-13].

The most detailed study of the formation of stable clusters of colloidal particles was undertaken for suspensions of polymethylmethacrilate monodisperse (polydispersity ≤ 5 %) spherical particles with mean radius in the range 212-777 nm in a mixture of cis-decalin and cycloheptyl bromide [3-9]. The matching densities allowed neglecting the influence of the gravity. The particles were positively charged in this dispersion medium. Non-adsorbing polymer polystyrene added to the dispersion medium provided the short range depletion attraction in the system with strength controlled by polymer concentration and molecular mass.

The presence of clusters in colloidal suspensions at equilibrium with single particles was observed at relatively low polymer concentrations and solid volume fractions [6]. An increase of both polymer concentrations and solid volume fractions resulted in the increase of the cluster size and finally in formation of gel-like structures [4-6]. Using the confocal microscopy allowed the clear visualisation of clustering [3-6]. According to [3] at polymer concentration 3 g/l and molecular mass 212.4 kDa, the equilibrium cluster aggregation number increased from about 3 at the solid volume fraction of φ=0.025 to more than 20 at the solid volume fraction of φ=0.15.

The stable cluster formation was also observed in aqueous suspensions of inorganic particles: of iron oxyhydroxide [10], sodium cloisite clay [11], and crystalline quartz [12] as well as in aqueous suspensions of influenza viruses [13]. Note, that clusters observed in [3-13] are very stable structures, as they did not show any noticeable growth during long periods of observation (from hundreds of hours to months).

The basic concept in explanation of stable cluster formation is the balance of competing forces between short range attraction, usually dispersion, van der Waals or depletion interactions, and long range repulsion, usually screened electrostatic forces.

One of the approaches adopted in the literature is the employment of capillarity approximation, where the clusters are treated as uniform droplets [14]. The driving force for the cluster growth in this approach is the decrease of the surface energy of the system whereas the stabilising factor is the Coulomb repulsion.

Another approach is based on the calculation of ground state energy depending on the number of particles in the cluster [15, 16]. The pair potential of the interparticle interaction was approximated as the sum of Lennard-Jones (attraction) and Yukava (repulsion) potentials. It was found that there is a minimum on the curve representing dependence of ground-state energy per particle on the number of particles in the cluster. That means that the clusters containing a certain number of particles (about 20 for the parameter set chosen in [16]) are thermodynamically stable in this case.

At the same time the concept of importance of long range electrostatic repulsion for the cluster formation conflicts with some experimental results, as, for example, in [9,12] the clusters were observed at salt concentrations high enough to eliminate any long range electrostatic repulsion. In [12] the cluster formation was

explained by competition between van der Waals attraction and structural repulsion, which are less sensitive to the salt concentration in comparison to electrostatic forces. It can be also assumed that not only the presence of the repulsion barrier enables the formation of stable clusters, but also the finite depth of the secondary potential well, comparable with the energy of the thermal energy kT. In this case the cluster equilibrium size distribution is the result of competition between aggregation due to colloidal attraction forces and fragmentation caused, in the absence of external forces, by Brownian motion of colloidal particles.

Computer simulations are widely used in theoretical treatment of the reversible aggregation of colloidal suspensions [17-19]. In [17] Monte Carlo simulations were carried out of an ensemble of diffusing particles. It was assumed that the diffusion coefficient is inversely proportional to the cluster radius, and the bonds between particles in the cluster can be broken with a probability depending on the bond energy and number of bonds per particle. Under those assumptions Monte Carlo simulation [17] enabled the prediction of the dynamics of cluster growth and their structure at different values of bond energy and volume fraction of particles in the suspension.

Another way to simulate the aggregation kinetics is the numerical solution of the population balance equations with appropriate aggregation and fragmentation kernels [18]. The mean cluster size was found to be proportional to the inverse of the bond break up probability. To improve the accuracy of the model parameters in [19] it was complemented by Brownian dynamic simulation of the behaviour of the ensemble of soft-core particles using the Langevin equations [19]. Simulations were performed for the volume fraction of particles $\varphi=0.001$ and different strength of attraction in approximation of Stokes hydrodynamic resistance to the particles motion.

Results obtained in [19] showed that the direct computer simulation of the evolution of the particle ensemble is a powerful tool for the comprehensive study of clustering processes. It reveals detailed information on the mechanism of cluster formation and main parameters controlling this process. However, the use of the Stokes equation for the hydrodynamic resistance is too approximate when clustering is considered. Indeed, to form a cluster particles must be drawn close together (within nanometer range), where the colloidal forces begin to act. It is well known, that the hydrodynamic interaction between particles becomes significant even at separations of order of their radius and increases rapidly at smaller separations [20]. The

hydrodynamic resistance in this case becomes significantly higher than that given by Stokes equation. Moreover, it is no longer a scalar constant but a tensor with components depending on the particle positions and velocities [21].

The aim of the present study is the direct computer simulation of the reversible coagulation of colloidal particles. Therefore an improved mathematical model for Brownian dynamic simulation of the reversible aggregation in the colloidal suspension is proposed below with detailed discussion on the validity of approximations and parameters used. The most challenging problem in the modelling of the reversible aggregation is, in our opinion, the correct simulation of residence time of a particle in the potential well. This can be checked by monitoring the mean residence time. As any mathematical model of colloid behaviour inevitably uses many approximations, one should be sure, that the mean residence time is reasonably accurately modelled and there are no artificial effects in the simulation. It is difficult to check the mean residence time itself during the simulation. Hence we have to select suitable parameters, which can be easily estimated and are related to the mean residence time. The escape of the particle from the potential well is determined by the relation between the depth of the potential well and the instantaneous value of the kinetic energy of the particle. Therefore, the mean kinetic energy of the particles is used below as the system control parameter. The constant value of the mean kinetic energy of the particles indicates that no artificial energy is created or dissipated in the system and therefore one can expect the correct description of the particle behaviour in the potential well. To correctly model the system kinetic energy the full Langevin equations, including the inertial terms are used below.

Mathematical statement of the model

The colloidal suspension under consideration below is built up by N mono-disperse spherical particles moving in two dimensions x and y. To describe the particles motion the Brownian dynamic approach is used, based on the well known Langevin equations [22]:

$$m\frac{dV_i}{dt} = -\sum_{j=1}^{2N}\varsigma_{ij}V_j + \sum_{j=1}^{2N}\alpha_{ij}f_j + \sum_{j=1}^{2N}F_{ij}\,, \qquad (1)$$

where i,j=1…2N, $m = \frac{4}{3}\pi a^3\left(\rho_p + 0.5\rho_l\right)$ is the mass of the particle (including the added mass), a is the radius of the particle, ρ_p is the density of the particle material,

ρ_l is the density of the suspending liquid, V is the particle velocity, ς_{ij} is the element of the hydrodynamic resistance matrix, $\hat{\alpha} f$ represents the Brownian forces, with f_i being a random quantity, normally distributed, with

$$\langle f_i \rangle = 0, \tag{2}$$

$$\langle f_i(t) f_j(t') \rangle = 2\delta_{ij}\delta(t-t'), \tag{3}$$

$\boldsymbol{F}$ represents the colloidal forces, see the definition of the matrix of Brownian coefficients, $\hat{\alpha}$, below.

The matrix of hydrodynamic resistance coefficients, $\hat{\varsigma}$, and matrix of Brownian coefficients, $\hat{\alpha}$, are related according to the fluctuation-dissipation theorem [23]:

$$\varsigma_{ij} = \frac{1}{kT}\sum_l \alpha_{il}\alpha_{lj}, \tag{4}$$

where k is the Boltzmann constant, T is the absolute temperature. It is possible to show that the fluctuation dissipation relation (4) is independent of the colloidal forces $\boldsymbol{F}$ in Eqs. (1)

For a single spherical particle in an unbounded liquid (or for particles, at the distances much larger than their size) ς is a scalar determined by the Stokes law:

$$\varsigma = 6\pi\mu a, \tag{5}$$

where μ is the dynamic viscosity of the suspending liquid.

When particles approach each other the flow field caused by their motion acts upon other particles and $\hat{\varsigma}$ becomes a symmetric matrix. It is assumed below that all forces, including hydrodynamic forces, are pairwise additive, and for any pair of particles the hydrodynamic interaction depends only on distance between them and their relative velocities:

$$F_{H1} = -\varsigma_x(V_1 - V_3), \tag{6}$$

$$F_{H2} = -\varsigma_y(V_2 - V_4), \tag{7}$$

where F_{H1}, F_{H2} are the hydrodynamic force components acting on the particle 1 in the particle pair local co-ordinate, where axis x is parallel to the line connecting the particle centres, y is in the tangential direction. Note, V_1 and V_2 are x and y velocity components of particle 1, V_3 and V_4 are x and y velocity components of particle 2. It is assumed that the effects of particle rotation can be neglected.

The equations proposed by Cox [24] are used to calculate the coefficients ς_x and ς_y at the small separation between the particles surfaces $h \le 0.1a$:

$$\varsigma_x = \frac{3}{2}\pi\mu\frac{a^2}{h}, \qquad \text{at } h \le 0.1a, \tag{8}$$

$$\varsigma_y = \pi\mu a \ln\left(\frac{a}{h}\right), \qquad \text{at } h \le 0.1a. \tag{9}$$

Calculation of a logarithmic function is time consuming in numerical simulations, therefore the following approximation of Eq. (9) is used:

$$\varsigma_y = -\pi\mu a\left(1.8043 + 0.05\frac{a}{h} - 3\cdot 10^{-6}\frac{a^2}{h^2}\right), \qquad \text{at } h \le 0.1a. \tag{9a}$$

It is assumed that the hydrodynamic interaction becomes negligible at $h > 2.5a$. The interaction forces for $0.1a \le h \le 2.5a$ were fitted to enable a smooth transition between forces at $h \le 0.1a$ and 0 at $h = 2.5a$.

Taking into account Eqs. (5-7) the matrix of hydrodynamic resistance for two interacting particles can be written as follows:

$$\hat{\varsigma} = \begin{pmatrix} \varsigma + \varsigma_x & 0 & -\varsigma_x & 0 \\ 0 & \varsigma + \varsigma_y & 0 & -\varsigma_y \\ -\varsigma_x & 0 & \varsigma + \varsigma_x & 0 \\ 0 & -\varsigma_y & 0 & \varsigma + \varsigma_y \end{pmatrix} \tag{10}$$

i.e. it contains the only 4 different elements ς_x, ς_y, $\varsigma + \varsigma_x$ and $\varsigma + \varsigma_y$. The matrix of Brownian coefficients has the same form as the matrix of hydrodynamic coefficients (see Appendix):

$$\hat{\alpha} = \begin{pmatrix} \alpha_{11} & 0 & \alpha_{13} & 0 \\ 0 & \alpha_{22} & 0 & \alpha_{24} \\ \alpha_{13} & 0 & \alpha_{11} & 0 \\ 0 & \alpha_{24} & 0 & \alpha_{22} \end{pmatrix}. \tag{11}$$

The corresponding coefficients of the latter matrix are found by solving the set of Eqs (4) for elements of matrices (10) and (11) as shown in Appendix:

$$\begin{aligned} \alpha_{11} &= \frac{1}{2}\sqrt{kT}\left(\sqrt{\varsigma} + \sqrt{\varsigma + 2\varsigma_x}\right) \\ \alpha_{13} &= \frac{1}{2}\sqrt{kT}\left(\sqrt{\varsigma} - \sqrt{\varsigma + 2\varsigma_x}\right) \\ \alpha_{22} &= \frac{1}{2}\sqrt{kT}\left(\sqrt{\varsigma} + \sqrt{\varsigma + 2\varsigma_y}\right) \\ \alpha_{24} &= \frac{1}{2}\sqrt{kT}\left(\sqrt{\varsigma} - \sqrt{\varsigma + 2\varsigma_y}\right) \end{aligned}. \tag{12}$$

Following [26, 27], the random functions f_i obeying Eq. (2,3) were modelled below as:

$$f_i = \sqrt{\frac{2}{dt}} R_{ND} \quad , \qquad (13)$$

where dt is the time step to be chosen for computer simulations, R_{ND} is a random number with a normal distribution (the mean value is equal to zero and standard deviation is equal to 1).

According to the Derjaguin approximation [1, 25] the colloidal force acting along the centre line between particles is equal to

$$F(h) = \pi a \int_h^\infty \Pi(h) dh \, , \qquad (14)$$

where $\Pi(h)$ is the disjoining pressure between corresponding flat interfaces. Eq. (14) is valid if $h_2 << a$, where h_2 is the range of surface forces action. The latter inequality is valid for particles $a \sim 1 \mu m$, which are under consideration below.

To simplify the calculations at this stage we model the disjoining pressure $\Pi(h)$ in the simplest possible way (see Fig. 1a), which still keeps the main features of the real disjoining pressure: presence of both repulsion and attraction as well as the presence of a potential well (see below). The distances between particles corresponding to the zeros of disjoining pressure, h_1 and h_2, distance corresponding to the minimum of disjoining pressure, h_0, and depth of the potential well, U_{min}, are used as parameters to describe the disjoining pressure curve:

$$\Pi = \frac{2U_{\min}}{\pi a R} \frac{h_1 - h}{h_1 - h_0}, \qquad 0 < h < h_0, \qquad (15a)$$

$$\Pi = \frac{2U_{\min}}{\pi a R} \frac{h_2 - h}{h_2 - h_0}, \qquad h_0 < h < h_2, \qquad (15b)$$

where $R = \frac{S^3}{3(h_1 - h_0)} + \frac{(h_2 - h_0)^2 - (h_1 - h_0)^2}{3} + (h_2 - h_1)(S + h_0 - h_1)$ and

$S = \sqrt{(h_0 - h_1)(h_2 - h_1)}$.

According to Derjaguin's approximation (14) the interparticle force, F, (Fig. 1b) is as follows:

$$F = \frac{U_{\min}}{R} \left[\frac{(h_1 - h)^2}{h_1 - h_0} + h_2 - h_1 \right], \qquad 0 < h < h_0, \qquad (16a)$$

$$F = \frac{U_{\min}}{R}\frac{(h_2 - h)^2}{h_2 - h_0}, \qquad h_0<h<h_2, \qquad (16b)$$

and the interaction energy $U(h) = \int_h^\infty F(h)dh$ (Fig. 1c):

$$U = \frac{U_{\min}}{R}\left[\frac{(h_1 - h)^3}{3(h_1 - h_0)} + (h_2 - h_1)(h_0 - h) - \frac{(h_1 - h_0)^2 + (h_2 - h_0)^2}{3}\right], \quad 0<h<h_0, \quad (17a)$$

$$U = \frac{U_{\min}}{R}\frac{(h_2 - h)^3}{3(h_2 - h_0)}, \qquad h_0<h<h_2. \qquad (17b)$$

The curves presented in Fig. 1 are drawn for the following typical values $h_1=1.6\cdot10^{-6}$ *cm,* $h_2=3.0\cdot10^{-6}$ *cm,* $h_0=2.0\cdot10^{-6}$ *cm,* $U_{min}=10$ *kT*. Such an approximation for colloidal forces is a simplification, hence we plan to use more realistic data for interparticle interaction, obtained by direct Atomic Force Microscopy measurements of colloidal forces between particles in the future. Note, the simplified form of the disjoining pressure adopted above allows us to draw a number of important qualitative conclusions (see below).

Eqs (1) were solved by the finite difference Euler's method using the approximation of pairwise additivity of forces and taking into account the interaction of a particle with nearest neighbours (with centre-to centre distance $<4\cdot(a+h_2)$). Periodic boundary conditions were imposed on the whole system to simulate the behaviour of an unbounded colloidal suspension. A random initial distribution of particles over the 2-D lattice was used. The initial particles velocities, V_i, were generated according to the Maxwell distribution.

Results and discussions

Selection of the time step

According to [26] the Langevin equations (1) are applicable only if the correlation time for the Brownian force is much smaller, than the correlation time for momentum, t_p, to use correctly the model described in the previous section. If Brownian force is modelled as a stepwise function obeying Eq (13), the latter condition becomes [26]:

$$dt << t_p = \frac{m}{\varsigma}. \qquad (18)$$

In the case of a free moving particle in water ($\varsigma = 6\pi\mu a$) $t_p=3.3\cdot10^{-7}$ s and $dt=10^{-8}s$ seems to be a reasonable choice. Note, lower value of the time step should be used in the case of clustering due to higher hydrodynamic interactions between particles at small separations. If the liquid has a higher viscosity the time step should also be reduced.

To investigate the influence of the choice of the time step, the mean value (over time) of the kinetic energy of a free moving particle was calculated. The calculated kinetic energy normalised by the thermal energy, kT, is presented in Fig. 2 (curves 1 and 2) as a function of the selected time step. These curves are consistent with the above discussion. At the viscosity of dispersion medium of 1 cP (pure water or aqueous solutions) the normalised kinetic energy of the free moving particle approaches unity (theoretically correct) if the time step $dt<10^{-7}$ s. At a tenfold higher viscosity of the dispersion medium the time step should be decreased to $dt<10^{-8}$ s, to keep the normalised kinetic energy of particle close to 1. During clustering the distance between particles becomes very small and therefore, the hydrodynamic resistance increases considerably (about 10 times higher than predicted by Stokes law). Hence, the time step $dt=10^{-9}$ s was chosen in our simulations below, as a compromise between accuracy and runtime. The normalised mean value of the kinetic energy of each particle was monitored in our simulations, as a control parameter.

Influence of inertia

Frequently the diffusion approximation is used for the computer simulation of the motion of the Brownian particles. The advantage of this approximation is the possibility (i) of using a time step which is much larger than the momentum relaxation time and (ii) neglecting the inertial term in the Langevin equations (1) [21,23]. These simplify the calculations considerably providing nevertheless correct enough simulation results. However, Fig. 2 (curve 3) shows that neglecting the inertial term results in a strong dependency of the simulated value of the mean particle energy on the time step chosen. At $dt>10^{-6}$ s the simulated value of the particles kinetic energy becomes negligible compared to kT. That means, that in diffusion approximation the particles velocities calculated using Eqs (1) should be considered as formal parameters only (velocities of a diffusional drift), which have no relation to the particles kinetic energies. Therefore, the latter approximation does not allow the particles kinetic energy to be used as the system control parameter.

Diffusion coefficient

For further validation of the proposed mathematical model, the diffusion coefficient of a single particle freely moving in water was calculated according to the following equation [22]:

$$D = \frac{\left\langle (x - x_0)^2 + (y - y_0)^2 \right\rangle}{4t}, \qquad (19)$$

where x_0 and y_0 are the initial co-ordinates of the particle, x and y its co-ordinates at time $t>>t_p$, averaging is performed over the ensemble of particles. Below D is normalised by the theoretical value

$$D_0 = \frac{kT}{6\pi\mu a}. \qquad (20)$$

The results of computer simulations of diffusion coefficient are presented in Fig. 3 as a function of the number of ensembles over which the averaging was performed. Fig. 3 shows that the computer simulations predict the correct value of the diffusion coefficient. Note, that computer simulations performed using the diffusion approximation neglecting the inertial term also predict the correct value of the diffusion coefficient.

Residence time in the potential well

The mathematical model described above correctly models the particles kinetic energy, hence, it is expected that this model should also correctly describe particle motion under the action of colloidal forces without the introduction of extra parameters, such as a probability of bond breakage [17].

Let us consider pair of interacting particle. The latter means that there is only one particle in the potential well. Then the probability of escape of that particle from the potential well can be calculated using the Smoluchowski equation for the flux of particles in the field of force $F(x)=-dU/dx$ [28]:

$$j = \frac{1}{\varsigma_{11}} Fw - D\frac{dw}{dx} = -\frac{1}{\varsigma_{11}}\frac{dU}{dx}w - \frac{kT}{\varsigma_{11}}\frac{dw}{dx}, \qquad (21)$$

where j is the particles steady state flux, s^{-1}, $w(x)$ is the particles probability distribution function, cm^{-1}, D is the particles diffusion coefficient, ς_{11} is determined by Eqs (5), (8) and (10), and $U(x)$ is given by Eq. (17).

Eq. (21) should be solved with the following boundary conditions:

$$w(h_2) = 0 \qquad (22)$$

and

$$\int_0^{h_2} w(x)dx = 1\,. \qquad (23)$$

The first boundary condition (22) means that all particles disappear from the potential well after reaching the end of the zone where the surface forces act. The second boundary condition (23) means that precisely one particle is located in the zone of the surface forces action. Direct solution of Eq. (21) with two boundary conditions (22) - (23) and taking into account that $D=kT/\varsigma_{11}$ results in the following expression for the mean particle residence time in the potential well:

$$\bar{t}_R = \frac{1}{j} = \frac{\left(\int_0^{h_2} \exp\left(-\frac{U(x)}{kT}\right)dx \int_x^{h_2} \varsigma_{11}(x')\exp\left(\frac{U(x')}{kT}\right)dx'\right)}{kT}\,. \qquad (24)$$

The mean residence times in the potential well calculated according to Eq.(24) are presented in Table 1 (the second row) and compared with results of the computer simulations according to the model based on Eq. (1) taking the inertia into account (the third row) and according to the diffusional approximation described by Eq. (15) in Ref [23] neglecting the inertial term in Langevin equations (the fourth row). The simulated mean residence times were obtained in the following way. Two particles were placed initially at the distance corresponding to the minimum of the potential well and simulation of their relative motion was performed until the instant, when the distance between particles exceeded the range of colloidal interaction, h_2. The mean residence time was calculated from 20 simulations for each potential well depth for the model Eq. (1) and from 40 simulations for the model of Ref [23].

Table 1

The potential well depth, kT	1	3	5	7
The mean residence time calculated according to Eq.(24), s	0.044	0.12	0.50	2.7
The mean residence time obtained by direct computer simulations according to Eq. (1), s	0.024	0.11	0.46	2.4
The mean residence time obtained by direct computer simulations according to Eq. (15) in Ref [23], s*	0.048	0.11	0.55	2.8

*Simulations were performed with the time step $dt=10^{-6}$ s.

Table 1 shows that the results of the computer simulation performed according to Eq. (1) are very close to those obtained by diffusion approximation and the both simulations results are in good agreement with those calculated using Eq. (24). Eq. (1) slightly underestimates the residence time because at the selected time step the mean kinetic energy of particles was overestimated by about 3 %. Such an artificial increase of the kinetic energy is more significant for smaller potential well depth as can be noticed from Table 1: there is more significant difference between simulated and analytical results at the potential well depth equal to 1 kT. The results presented in Table 1 confirm that the presented mathematical model, as well as diffusional model proposed in Ref [23] enable the simulation of clustering behaviour based solely on first principles without any empirical fit. The drawback of the presented model in comparison to diffusion approximation is much smaller time step. However, the presented model allows monitoring the energy of each particle during the simulation process and therefore it can be used as a reference model to verify the validity of the numerical scheme providing further simulations employing diffusion approximation.

Behaviour of clusters

The behaviour of a small cluster composed of 4 colloidal particles, simulated using the above model is presented in Fig. 4. Initially each particle was located in the potential wells of its two nearest neighbours. The cluster breaks very quickly in the absence of colloidal interactions. For 4 kT potential well depth the cluster also disaggregates relatively quickly, but one doublet remains unbroken even after 4 s. At a larger potential well depth, 10 kT, the cluster remains stable, with particles moving tangentially inside the cluster, which changes slowly its shape.

A computer simulation for a larger system, composed of 170 particles, was also performed. Initially particles were randomly distributed over a 2D lattice, but far enough from each other to ensure no particle interactions. The particle volume fraction selected was about 30% as shown in Fig. 5a. The changes in the system configuration over 20s were then simulated for two cases: (i) in the absence of colloidal interactions. In this case the particles become redistributed more uniformly over the available 2D space (Fig. 5b), (ii) at strong colloidal interactions (potential well depth of 20 kT). In this case the particles combined into clusters (Fig. 5c), i.e. in

this case the computer simulation allows observation of the onset of the coagulation process.

Conclusions

The self consistent mathematical model of the behaviour of colloidal suspensions based on the Langevin equations and pairwise interaction between colloidal particles can provide quantitative information on clustering in colloidal suspensions. Calculations based on this model yield valid energies, particle diffusion coefficients and residence times of colloidal particles inside the potential well. That means, that in the framework of this model, colloidal suspensions can be fully described using the Langevin equations only and theoretical hydrodynamic and colloidal interactions. The presented model allows monitoring the energy of each particle during the simulation process and therefore it can be used as a reference model to verify the validity of the numerical scheme for simulation using diffusion approximation.

The computer simulations performed using the proposed model enabled the monitoring of formation and breakage of clusters in a suspension caused by competing colloidal interactions and thermal particle motion. In the case of a very deep potential well the computer simulation showed an onset of the coagulation of the suspension as expected.

Acknowledgement

The authors would like to acknowledge the support from The Engineering and Physical Sciences Research Council, UK (Grant **EP/C528557/1**).

Appendix

Let us calculate the square of the matrix (11):

$$\hat{\alpha}^2 = \begin{pmatrix} \alpha_{11} & 0 & \alpha_{13} & 0 \\ 0 & \alpha_{22} & 0 & \alpha_{24} \\ \alpha_{13} & 0 & \alpha_{11} & 0 \\ 0 & \alpha_{24} & 0 & \alpha_{22} \end{pmatrix} \begin{pmatrix} \alpha_{11} & 0 & \alpha_{13} & 0 \\ 0 & \alpha_{22} & 0 & \alpha_{24} \\ \alpha_{13} & 0 & \alpha_{11} & 0 \\ 0 & \alpha_{24} & 0 & \alpha_{22} \end{pmatrix} =$$

$$= \begin{pmatrix} \alpha_{11}^2 + \alpha_{13}^2 & 0 & 2\alpha_{11}\alpha_{13} & 0 \\ 0 & \alpha_{22}^2 + \alpha_{24}^2 & 0 & 2\alpha_{22}\alpha_{24} \\ 2\alpha_{11}\alpha_{13} & 0 & \alpha_{11}^2 + \alpha_{13}^2 & 0 \\ 0 & 2\alpha_{22}\alpha_{24} & 0 & \alpha_{22}^2 + \alpha_{24}^2 \end{pmatrix}, \quad (1A)$$

The latter shows that $\hat{\alpha}^2$ and the resistance matrix $\hat{\varsigma}$ (10) have the identical structure. Substituting expressions (1A) and (10) in Eq. (4) one obtains the following set of equations for unknown values α_{ij}:

$$\begin{cases} \alpha_{11}^2 + \alpha_{13}^2 = kT(\varsigma + \varsigma_x) \\ 2\alpha_{11}\alpha_{13} = -kT\varsigma_x \\ \alpha_{22}^2 + \alpha_{24}^2 = kT(\varsigma + \varsigma_y) \\ 2\alpha_{22}\alpha_{24} = -kT\varsigma_y \end{cases}. \quad (2A)$$

Adding and subtracting equations 1 and 2 as well as equations 3 and 4 in the system of equation (2A) we conclude:

$$\begin{cases} (\alpha_{11} + \alpha_{13})^2 = kT\varsigma \\ (\alpha_{11} - \alpha_{13})^2 = kT(\varsigma + 2\varsigma_x) \\ (\alpha_{22} + \alpha_{24})^2 = kT\varsigma \\ (\alpha_{22} - \alpha_{24})^2 = kT(\varsigma + 2\varsigma_y) \end{cases}. \quad (3A)$$

Selecting the positive roots for $\alpha_{11} + \alpha_{13}$, $\alpha_{22} + \alpha_{24}$ and taking into account that $|\alpha_{11}| > |\alpha_{13}|$, $|\alpha_{22}| > |\alpha_{24}|$ we arrive to Eq. (12).

References

1. Deryaguin, B.V., Churaev, N.V., and Muller, V.M. "Surface forces", Consultants Bureau, Plenum Press, New York, 1987.
2. "Colloid science. Principles, methods and applications". Ed. By T. Cosgrove, Oxford: Blackwell, 2005.
3. Stradner A., Sedgwick H., Cardinaux F., Poon, W.C.K., Egelhaaf S.U., and Schurtenberger P. Equilibrium cluster formation in concentrated protein solutions and colloids. *Nature*, 2004, **432**, 492.
4. Dinsmore A.D., and Weitz D.A. Direct imaging of three-demensional structure and topology of colloidal gels. *J. Phys.: Condens. Matter*, 2002, **14**, 7581.
5. Campbell A.I., Anderson V.J., van Duijneveldt J.S., and Bartlett P. Dynamical arrest in attractive colloids: the effect of long-range repulsion. *Phys. Rev. Letters*, 2005, **94**, 208301.
6. Sedgwick H., Egelhaaf S.U., and Poon, W.C.K. Clusters and gels in systems of sticky particles. *J. Phys.: Condens. Matter*, 2004, **16**, S4913.
7. Segre P.N., Prasad V., Schofield A.B., and Weitz D.A. Glasslike kinetic arrest at the colloidal-gelation transition. *Phys. Rev. Letters*, 2001, **86**, 6042.
8. Sanchez R., and Bartlett P. Equilibrium cluster formation and gelation. *J. Phys.: Condens. Matter*, 2005, **17**, S3551.
9. Lu P.J., Conrad J.C., Wyss H.M., Schofield A.B., and Weitz D.A. Fluids of clusters in attractive colloids. *Phys. Rev. Lett*., 2006, **96**, 028306.
10. Gilbert B., Lu G., and Kim C.S. Stable cluster formation in aqueous suspensions of iron oxyhydroxyde nanoparticles. *J. Coll. Int. Sci*., 2007, **313**, 152.
11. Shalkevich A., Stradner A., Bhat S.K., Muller F., and Schurtenberger P. Cluster, glass, and gel formation and viscoelastic phase separation in aqueous clay suspensions. *Langmuir,* 2007, **23**, 3570.
12. Golikova E.V., Chernoberezhskii Yu.M., Grigor'ev V.S., and Semenov M.P. Aggregate stability of the sol prepared from crystalline quartz in aqueous solutions of potassium chloride. *Glass Physics and Chemictry*, 2006, **32**(6), 646.

13. Molodkina L.M., Golikova E.V., Chernoberezhsky Yu.M., and Kolikov V.M. Flow ultramicroscopy investigation of the aggregate stability of influenza virus dispersions. *Coll. & Surf. A,* 1995, **98**, 1.
14. Groenewold J., and Kegel W.K. Anomalously large equilibrium clusters of colloids. *J. Phys. Chem. B,* 2001, **105**, 11702.
15. Sciortino F., Mossa S., Zaccareli E., and Tartaglia P. Equilibrium cluster phases and low-density arrested disordered states: the role of short-range attraction and long-range repulsion. *Phys. Rev. Lett.,* 2004, **93**, 055701.
16. Mossa S., Sciortino F., Tartaglia P., and Zaccareli E. Ground-state clusters for short-range attractive and long-range repulsive potentials. *Langmuir*, 2004, **20**, 10756.
17. Haw M.D., Sievwright M., Poon W.C.K, and Pusey P.N. Cluster-cluster gelation with finite bond energy. *Adv. Coll. Int. Sci*., 1995, **62**, 1.
18. Odrizola G., Schmitt A., Moncho-Jorda A., Callejas-Fernandez J., Martinez-Garcia R., Leone R., and Hidalgo-Alvarez R. Constant bond breakup probability model for reversible aggregation processes. *Phys. Rev. E*, 2002, **65**, 031405.
19. Puertas A.M., and Odrizola G. Linking phase behaviour and reversible colloidal aggregation at low concentrations: simulations and stochastic mean field theory. *J. Phys. Chem. B*, 2007, **111**, 5564.
20. Happel J., Brenner H. "Low Reynolds number hydrodynamics with special applications to particulate media". Prentice-Hall, 1965.
21. Ball R.C., and Melrose J.R. A simulation technique for many spheres in quasi-static motion under frame-invariant pair drag and Brownian forces. *Physica A,* 1997, **247**, 444-472.
22. Coffey W.T., Kalmykov Yu.P., and Waldron J.T. The Langevin equation. With applications in physics, chemistry and electrical engineering. World scientific series in contemporary chemical physics. Vol. 11., World scientific publishing 1996.
23. Ermak D.L., and McCammon J.A. Brownian dynamics with hydrodynamic interactions. *J. Chem. Phys*., 1978, **69**, 1352.
24. Cox R.G. The motion of suspended particles almost in contact. *Int. J. Multiphase Flow,* 1974, **1**, 343.

25. Israelachvili J.N. “Intermolecular and surface forces”, Academic Press, London, 1992.
26. Turq P., Lanteime F., and Friedman H.L. Brownian dynamic: its application to ionic solutions. *J. Chem. Phys*., 1977, **66**, 3039.
27. Groot R.D., and Warren P.B. Dissipative particle dynamics: Bridging the gap between atomistic and mesoscopic simulation. *J. Chem. Phys.,* 1997, **107**, 4423.
28. Chandrasekhar S. Stochastic problems in physics and astronomy. *Reviews Modern Physics,* 1943, **15**, 1.

Figure legends

Fig. 1. Colloidal interaction between particles used in the computer simulations: a – disjoining pressure, b – force of interaction, c – interaction energy. The selected values of parameters are: $h_1=1.6\cdot10^{-6}$ *cm,* $h_0=2.0\cdot10^{-6}$ *cm,* $h_2=3.0\cdot10^{-6}$ *cm,* $U_{min}=10$ *kT.*

Fig. 2. Normalised mean kinetic energy of a single free moving particle vs the time step used in computer simulations:

1 liquid viscosity $\mu=1$ *cP;*

2 liquid viscosity $\mu=10$ *cP;*

3 liquid viscosity $\mu=1$ *cP*. The inertia term in Eq.(1) is neglected.

Fig. 3. Normalised diffusion coefficient of a single particle on the number of ensembles used for averaging.

Fig. 4. Time evolution of ensemble of 4 colloidal particles depending on the depth of the potential well of colloidal forces. Initially particles are located at separations corresponding to the minimum of the potential well: a – without colloidal interaction, b – $U_{min}=4kT$, c – $U_{min}=10kT$. Radius of the particles $a=10^{-4}$ *cm.*

Fig. 5. Structure formation in colloidal suspension (170 particles): a – initial random particle distribution; b – structure after 20 s without colloidal interaction, c – structure after 20 s with colloidal interaction potential well depth of 20 kT. Radius of the particles $a=10^{-4}$ *cm.*

List of symbols

Roman

a – the radius of the particle

dt – the time step chosen for computer simulations

D – the diffusion coefficient

D_0 – the diffusion coefficient of freely moving single particle

f_i – a random quantity representing the Brownian force

F – the colloidal force between two particles

F_H – the force of the hydrodynamic interaction between two particles

h – the distance between the particles surfaces

h_0 – the distances between the surfaces of the two particles where disjoining pressure has the minimum

h_1, h_2 – the distances between the surfaces of the two particles where disjoining pressure is equal to zero

j – the steady state particles flux from the potential well

k – the Boltzmann constant,

m – the mass of the particle

R_{ND} – a random number from normal distribution with mean equal to zero and standard deviation equal to 1

R, S – parameters in equations describing colloidal interaction between two particles

t – time

t_p – the correlation time for momentum

$\bar{t}_R$ – the mean time of a particle residence in the potential well

T – the absolute temperature

U – the pair potential of the colloidal interaction between two particles

U_{min} – the minimum of the pair potential

V – the particle velocity

w – the particles probability distribution function inside the potential well

x,y – the coordinates

x_0, y_0 – the initial co-ordinates of the particle (at $t=0$)

Greek

$\hat{\alpha}$ – the matrix of the Brownian coefficients

α_{ij} – the element of the Brownian coefficients matrix

μ – the dynamic viscosity of the suspending liquid

Π – disjoining pressure between two particles

ρ_l – the density of the suspending liquid

ρ_p – the density of the particle material

$\hat{\varsigma}$ – the matrix of the hydrodynamic resistance

ς – the hydrodynamic resistance for the single particle (according to the Stokes law)

ς_x – the hydrodynamic resistance due to motion of two particles along the centre-to centre line

ς_y – the hydrodynamic resistance due to motion of two particles transversely to the centre-to centre line

ς_{ij} – the element of the hydrodynamic resistance matrix

Figures

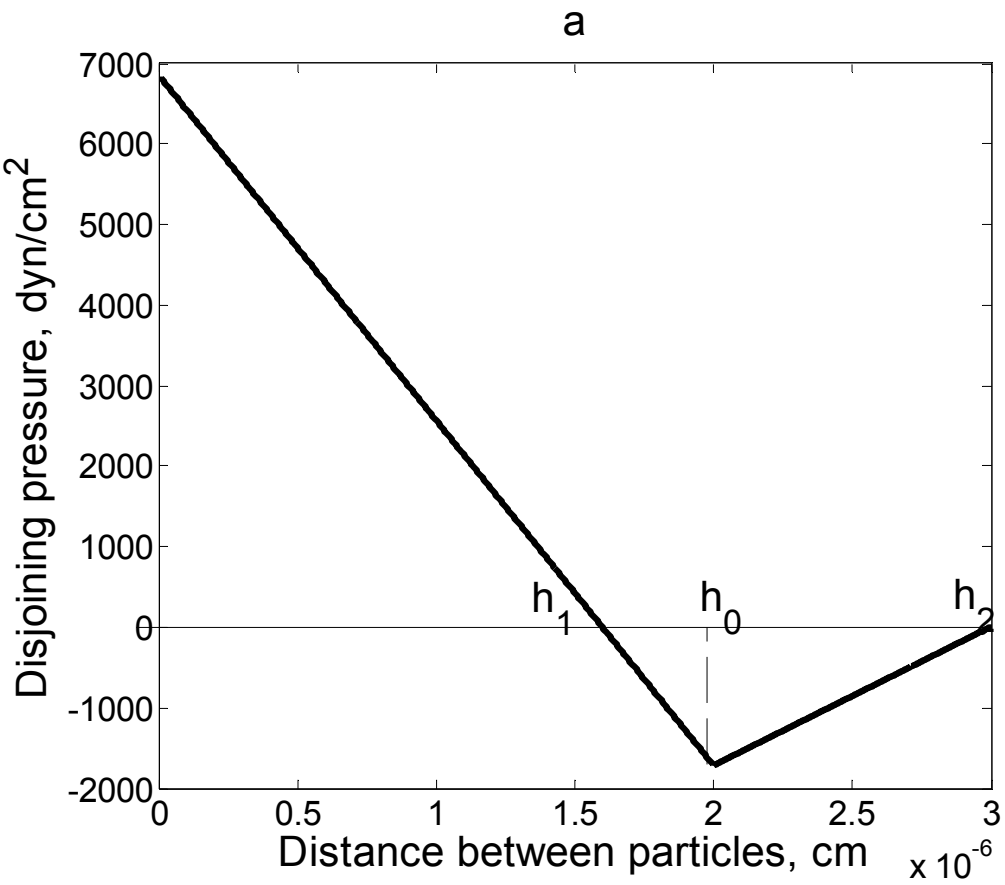

Fig. 1a

Fig. 1. Colloidal interaction between particles used in the computer simulations: a – disjoining pressure, b – force of interaction, c – potential of interaction. The selected values of parameters are: $h_1=1.6\cdot10^{-6}$ *cm*, $h_0=2.0\cdot10^{-6}$ *cm*, $h_2=3.0\cdot10^{-6}$ *cm*, $U_{min}=10$ *kT*.

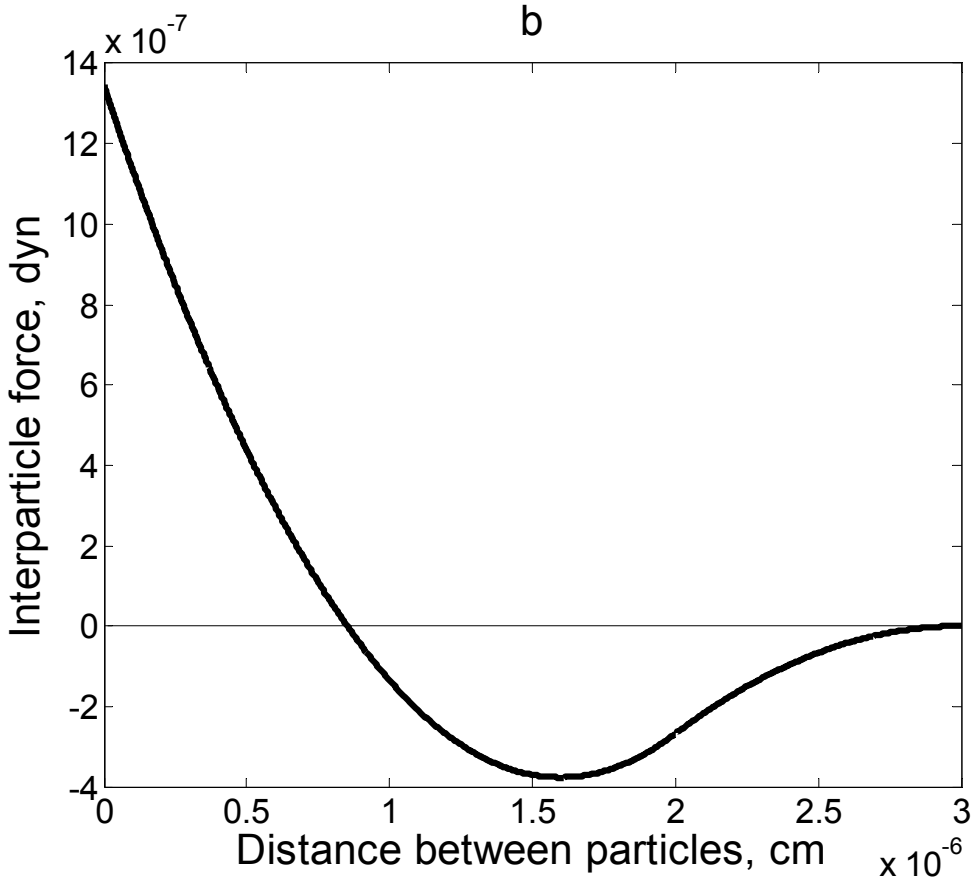

Fig 1b

Fig. 1. Colloidal interaction between particles used in the computer simulations: a – disjoining pressure, b – force of interaction, c – potential of interaction. The selected values of parameters are: $h_1=1.6\cdot10^{-6}$ *cm*, $h_0=2.0\cdot10^{-6}$ *cm*, $h_2=3.0\cdot10^{-6}$ *cm*, $U_{min}=10$ *kT*.

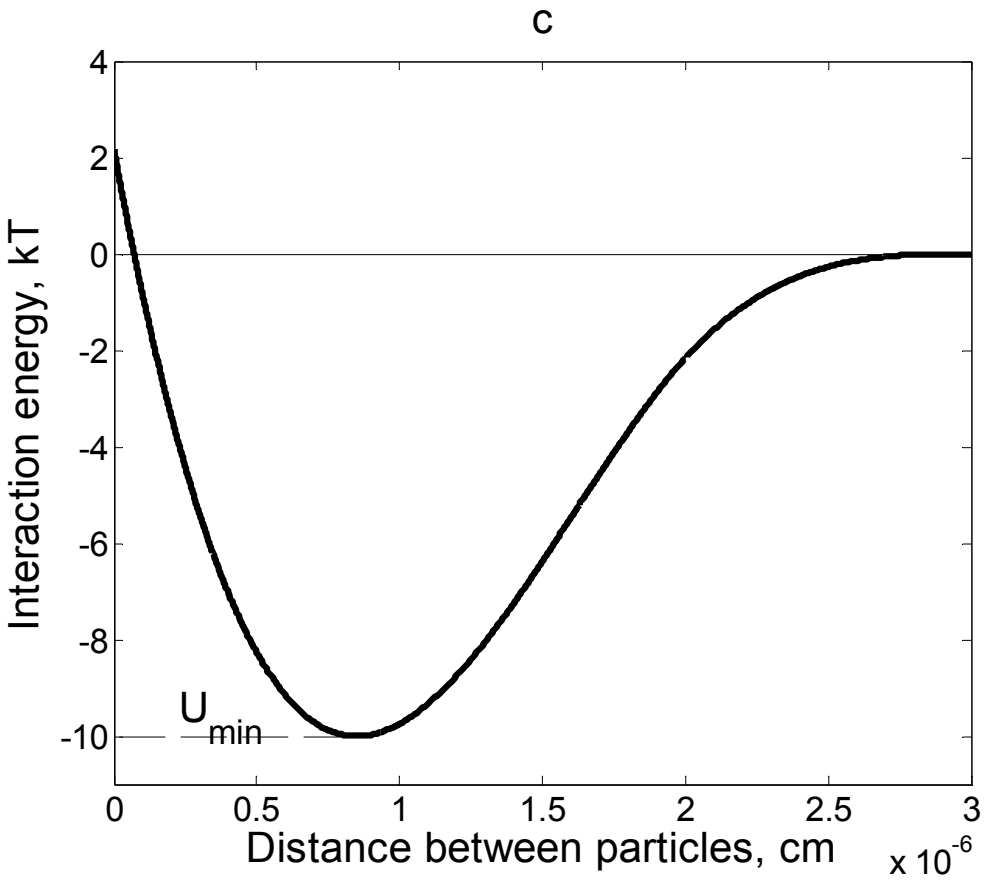

Fig. 1c

Fig. 1. Colloidal interaction between particles used in the computer simulations: a – disjoining pressure, b – force of interaction, c – potential of interaction. The selected values of parameters are: $h_1=1.6\cdot10^{-6}$ *cm*, $h_0=2.0\cdot10^{-6}$ *cm*, $h_2=3.0\cdot10^{-6}$ *cm*, $U_{min}=10$ *kT*.

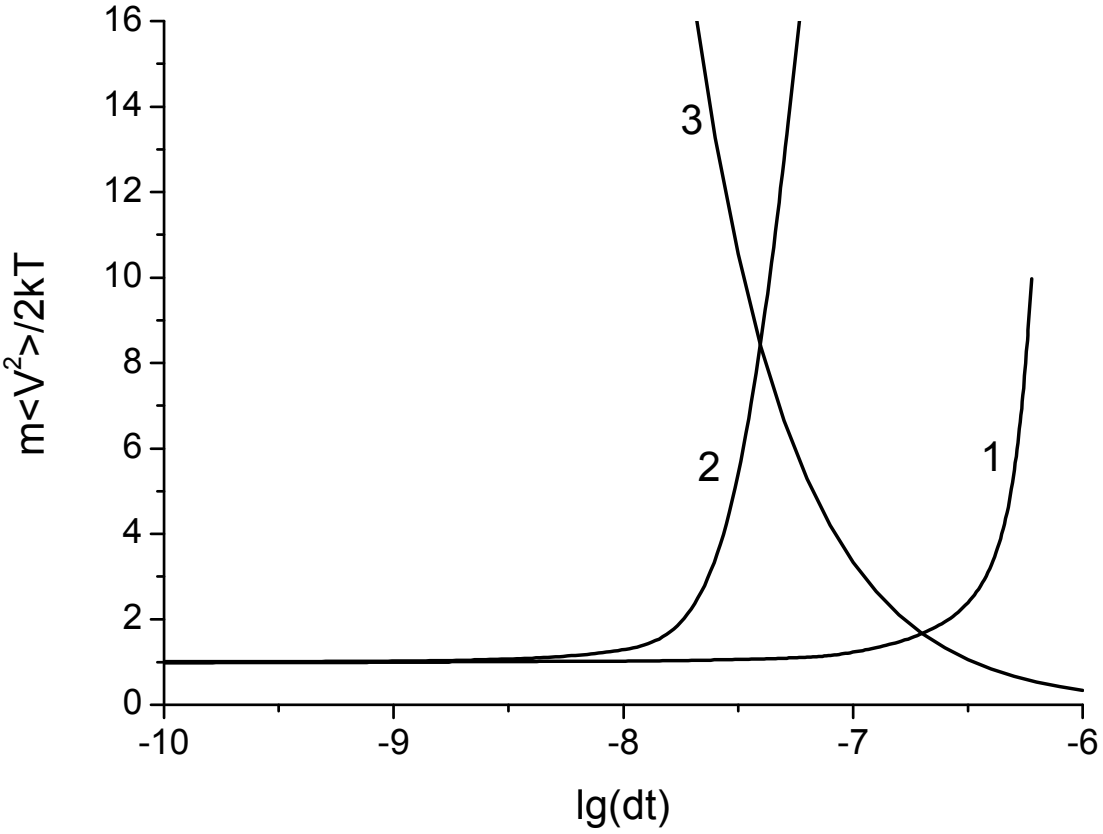

Fig. 2. Normalised mean kinetic energy of a single free moving particle vs the time step used in computer simulations:

1 liquid viscosity μ*=1 cP;*

2 liquid viscosity μ*=10 cP;*

3 liquid viscosity μ*=1 cP*. The inertial term in Eq.(1) is neglected.

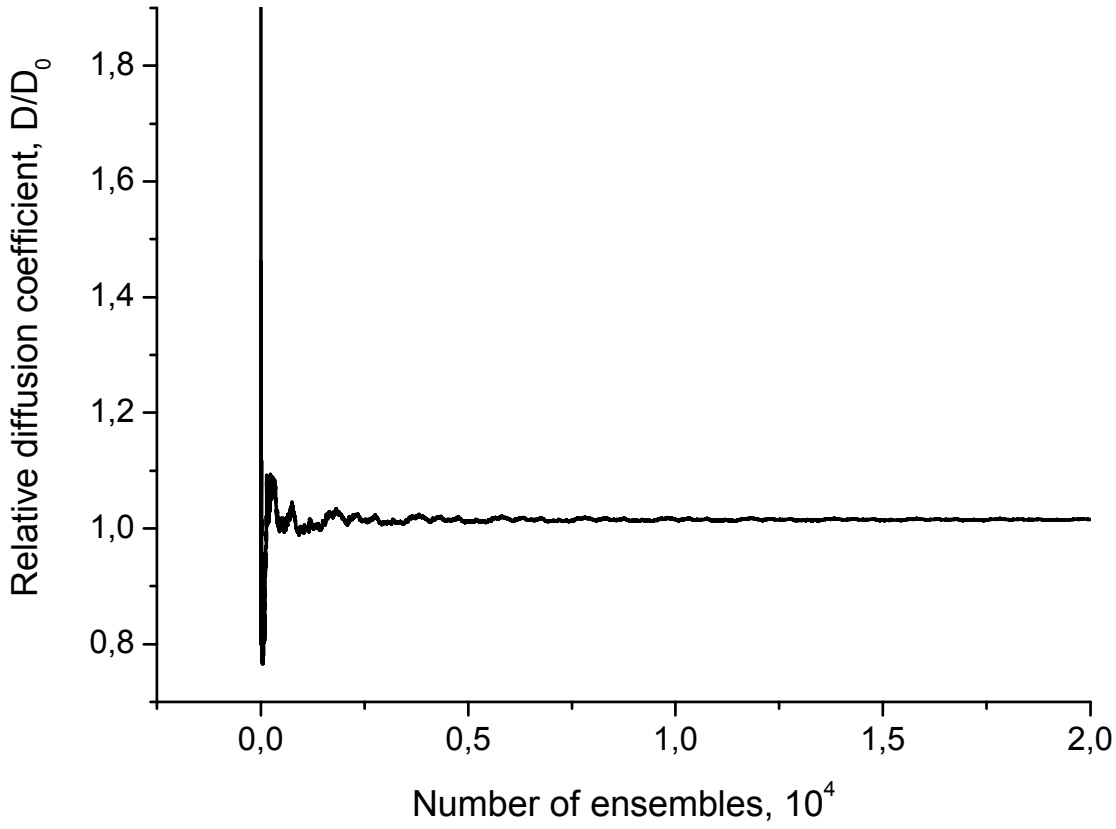

Fig. 3. Normalised diffusion coefficient of a single particle on the number of ensembles used for averaging.

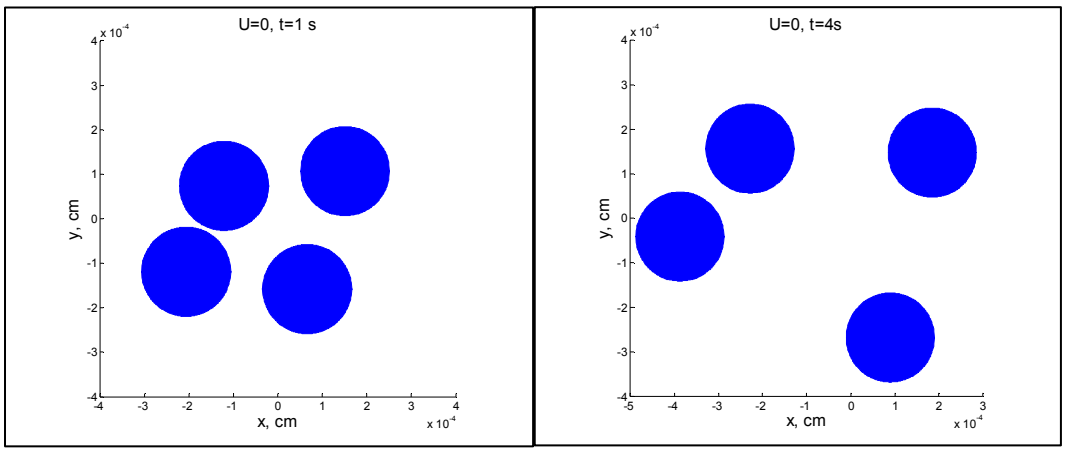

Fig. 4a

Fig. 4. Time evolution of ensemble of 4 colloidal particles depending on the depth of the potential well of colloidal forces. Initially particles are located at separations corresponding to the minimum of the potential well: a – without colloidal interaction, b – $U_{min}=4kT$, c – $U_{min}=10kT$. Radius of the particles a=10^{-4} cm.

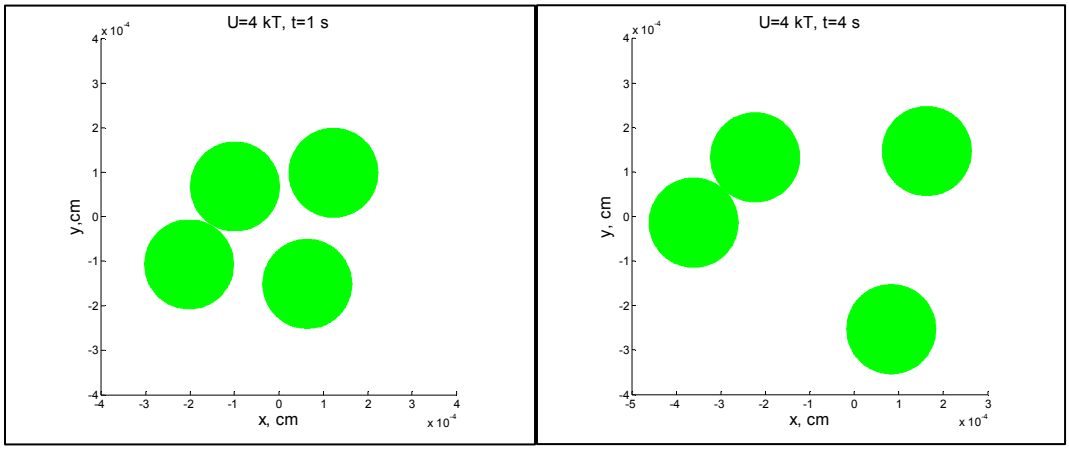

Fig. 4b

Fig. 4. Time evolution of ensemble of 4 colloidal particles depending on the depth of the potential well of colloidal forces. Initially particles are located at separations corresponding to the minimum of the potential well: a – without colloidal interaction, b – $U_{min}=4kT$, c – $U_{min}=10kT$. Radius of the particles a=10^{-4} cm.

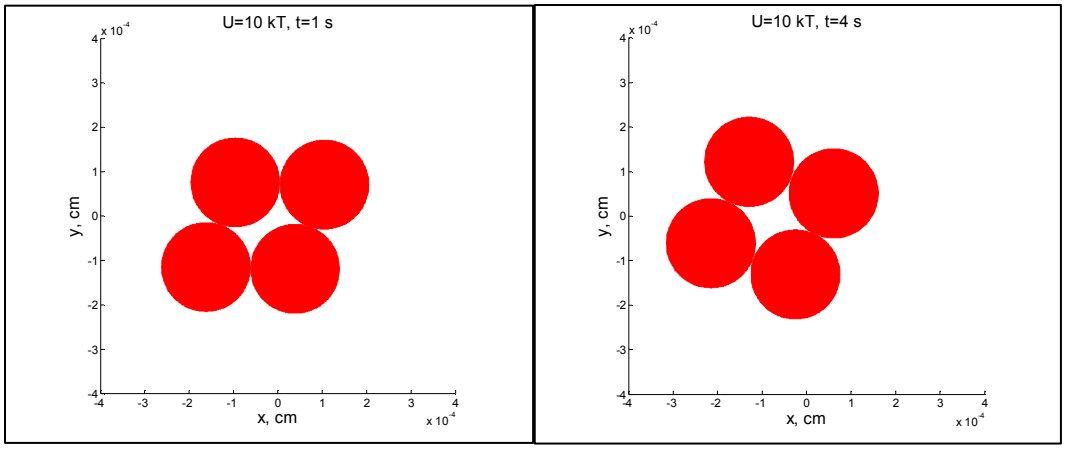

Fig. 4c

Fig. 4. Time evolution of ensemble of 4 colloidal particles depending on the depth of the potential well of colloidal forces. Initially particles are located at separations corresponding to the minimum of the potential well: a – without colloidal interaction, b – $U_{min}=4kT$, c – $U_{min}=10kT$. Radius of the particles a=10^{-4} cm.

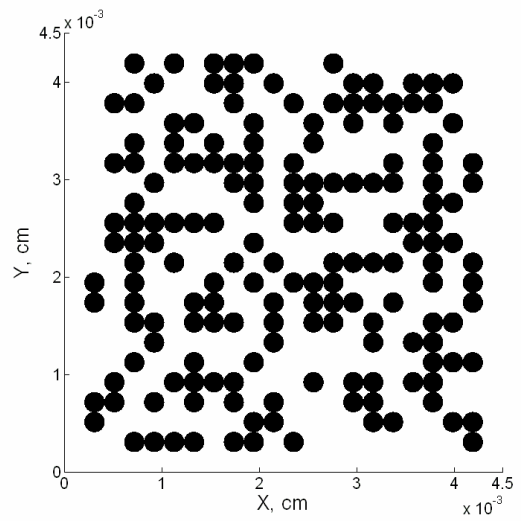

Fig. 5a

Fig. 5. Structure formation in colloidal suspension (170 particles): a – initial random particle distribution; b – structure after 20 s without colloidal interaction, c – structure after 20 s with colloidal interaction potential well depth of 20 kT. Radius of the particles $a=10^{-4}$ cm.

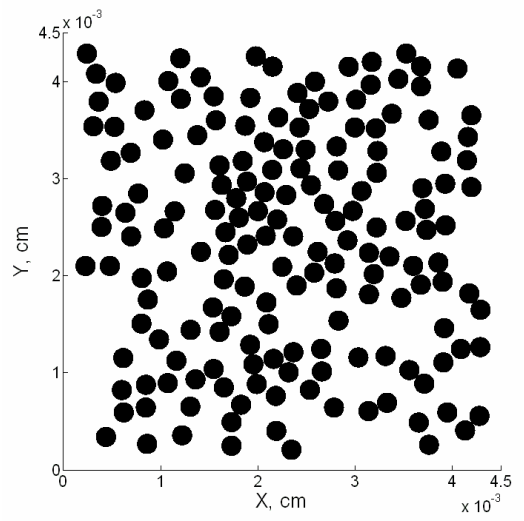

Fig. 5b

Fig. 5. Structure formation in colloidal suspension (170 particles): a – initial random particle distribution; b – structure after 20 s without colloidal interaction, c – structure after 20 s with colloidal interaction potential well depth of 20 kT. Radius of the particles $a=10^{-4}$ cm.

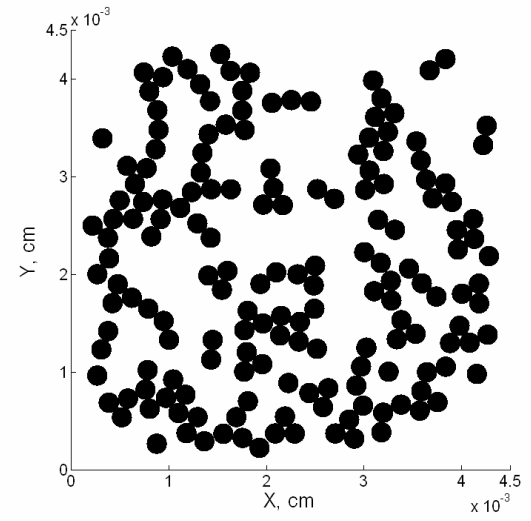

Fig. 5c

Fig. 5. Structure formation in colloidal suspension (170 particles): a – initial random particle distribution; b – structure after 20 s without colloidal interaction, c – structure after 20 s with colloidal interaction potential well depth of 20 kT. Radius of the particles $a=10^{-4}$ cm.